

Neutron diffraction from holographic polymer-dispersed liquid crystals

I. Drevensek-Olenik^a, M. A. Ellabban^b, M. Fally^b, K. P. Pranzas^c, J. Vollbrandt^c

^aFaculty of Mathematics and Physics, University of Ljubljana, Jadranska 19, and J. Stefan Institute, Jamova 39, Ljubljana, SI 1001, Slovenia

^bNonlinear Physics Group, Faculty of Physics, University of Vienna, Boltzmannngasse 5, Vienna, A-1090, Austria

^cInstitute for Materials Research, GKSS-Research Center Geesthacht GmbH, PO Box 1160, Geesthacht, 21494, Germany

ABSTRACT

Photopolymerization-induced phase separation of the constituent components in holographic polymer-dispersed liquid crystals (H-PDLCs) causes a huge variation of the refractive index for light as well as for neutrons. We demonstrated that H-PDLCs with the thickness of only 30 micrometers act as extremely efficient gratings for neutrons. The light-induced refractive-index modulation for neutrons of about 10^{-6} was observed, which is nearly two orders of magnitude larger than found in the best photo-neutron-refractive materials probed up to now. This makes H-PDLCs very promising candidate for fabricating neutron-optical devices.

Keywords: polymer-dispersed liquid crystals, holographic patterning, neutron diffraction, neutron-optical elements

1. INTRODUCTION

Holographic patterning in photosensitive polymers is usually associated with a spatial modulation of the density of the medium. Consequently upon illumination with light not only the refractive index for light, but also the refractive index for neutrons is modified¹. Such photo-neutron-refractive media provide a very convenient approach to fabricate neutron-optical devices for cold and ultra-cold neutrons, e.g. beam splitters, mirrors, lenses and interferometers. Large density modifications are expected in photosensitive mixtures, in which photochemical reaction processes are accompanied by phase separation of the constituent compounds. Examples of such materials are holographic polymer-dispersed liquid crystals (H-PDLCs).

H-PDLCs are electrically switchable photonic media fabricated by photopolymerization of a mixture of photosensitive monomers and liquid crystals (LCs) in the interference field of two or more laser beams^{2,3}. During photopolymerization reaction polymer molecules diffuse to the bright regions of the optical interference pattern, while liquid crystal molecules congregate in the dark regions⁴. This process is accompanied by a subsequent phase separation of the two media. As a result holographic gratings with extremely high refractive-index contrast for light are formed. In addition, the diffraction efficiency of these gratings is electrically switchable; application of an electric field results in reorientation of the nematic director field within the birefringent LC domains and consequently refractive-index mismatch between the LC regions and the polymer network is modified. Due to this property H-PDLCs are very promising candidates for applications in various electrooptic and display devices.

Reorientation of the nematic director field within the LC domains influences only the light-optical refractive index of the domains, but it does not affect the density of the LC medium. Also when LC domains undergo a transition from the nematic to the isotropic phase, their density remains practically constant. So to elucidate information on density

variations in a H-PDLC grating, optical diffraction measurements should be performed in the isotropic phase of the LC. On the contrary, the refractive index for neutrons is assumed to be independent of the molecular orientation and thus is insensitive to the nematic-isotropic (N-I) phase transition. According to these assumptions we performed a detailed analysis of the temperature dependence of the optical diffraction properties of a set of H-PDLC transmission gratings fabricated from commercially available constituents. The same gratings were then analyzed also by neutron diffraction experiments, which revealed an extremely high contrast of the refractive-index modulation for cold neutrons.

2. EXPERIMENTS

We used a material composition similar to that reported in the literature⁵. The samples were prepared from the UV curable emulsion containing 55 wt% of the LC mixture (TL203, Merck), 33 wt% of the prepolymer (PN393, Nematel) and 12 wt% of the 1,1,1,3,3,3-Hexafluoroisopropyl acrylate (HFIPA, Sigma-Aldrich). Standard cells made from two glass plates separated by $L = 50 \mu\text{m}$ thick Mylar spacers were filled with the optically isotropic mixture by means of the capillary flow. The samples were cured in the interference field of two expanded beams from an Argon ion laser operating at a wavelength of $\lambda_{UV} = 351 \text{ nm}$. The writing beams of equal intensity entered the sample symmetrically with respect to the sample normal, so that an unslanted transmission grating with the grating spacing of $\Lambda = 1.2 \mu\text{m}$ was recorded (Fig.). The total intensity of the writing beams during the writing process was 6 mW/cm^2 . The beams were linearly polarized along the y -axis. After recording the samples were postcured with a single laser beam for 105 seconds.

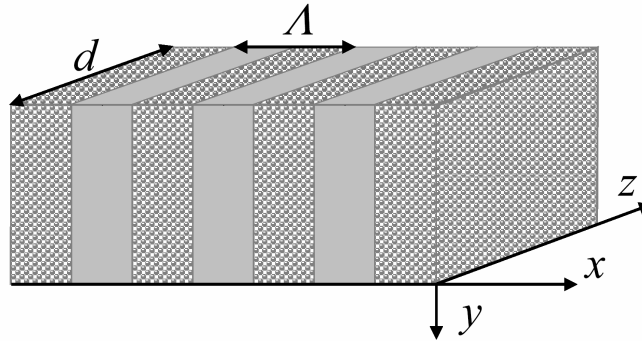


Fig. 1. Schematic drawing of the H-PDLC transmission grating of thickness d and grating spacing Λ .

The TL203 nematic liquid crystal mixture has a positive optical anisotropy with $n_a = n_{||} - n_{\perp} = 0.201$, where $n_{\perp} = 1.529$ is the ordinary and $n_{||} = 1.730$ is the extraordinary refractive index. It is composed of pentyl cyanobiphenyl (5CB) mixed with fluoro and chloro substituted mesogens. The bulk nematic-isotropic (N-I) phase transition of TL203 is at $74.6 \text{ }^{\circ}\text{C}$. The pre-polymer system PN393 is an ethylhexyl acrylate based mixture with a refractive index $n_p = 1.473$. The fluoro-additive (HFIPA), which is presumed to mediate anchoring properties at the polymer-LC interface, has the refractive index $n_f = 1.319$. All data are given for $\lambda_D = 589 \text{ nm}$. The densities of the constituent compounds are: $\rho_{PN393} = 0.912 \text{ g/cm}^3$, $\rho_{TL203} = 0.985 \text{ g/cm}^3$, and $\rho_{HFIPA} = 1.33 \text{ g/cm}^3$.

The sample was mounted to a heating stage, the temperature of which was controlled with an accuracy of $\pm 0.2 \text{ }^{\circ}\text{C}$. The heating stage was placed on a precise rotation stage with its rotation axis parallel to the y -axis of the grating (Fig. 1). Diffraction properties of the sample were probed by a He-Ne laser beam with the wavelength of $\lambda_R = 543 \text{ nm}$ and an optical power of 1 mW . The beam was expanded with a collimator, passed a pinhole with the diameter of 2 mm and was then sent to the sample. Three silicon photodiodes were used to simultaneously detect the intensity of the transmitted beam (0^{th} diffraction order) and the intensities of the two selected diffracted beams. To identify the N-I phase transition temperature the sample was at first slowly heated from room temperature to $T = 90 \text{ }^{\circ}\text{C}$ and the intensities of the 0^{th} and the $\pm 1^{\text{st}}$ diffraction orders were measured at a fixed orientation of the sample with respect to the probe beam. In the nematic phase all the intensities strongly vary with increasing temperature, while at $T_c = 68 \pm 0.2 \text{ }^{\circ}\text{C}$ they stabilize and do not change upon further heating. We hence assume that the N-I phase transition in our gratings takes place at $68 \text{ }^{\circ}\text{C}$. The value of T_c is down-shifted with respect to the pure LC, because of the presence of the polymer constituents within the

LC droplets, which is a known phenomenon in H-PDLCs. After identification of T_c , the angular dependence of the diffraction orders was measured at selected temperatures.

Small-angle neutron scattering experiments were performed at the SANS-2 instrument at the Geesthacht Neutron Facility (GeNF). The central neutron wavelength was $\lambda_n = 1.16$ nm or $\lambda_n = 1.96$ nm with a wavelength spread of $\Delta\lambda_n/\lambda_n = 10\%$. Full collimation distance (16 m) with two diaphragms of 5 mm width were used, so that the angular spread was < 1 mrad. The diffracted neutrons were collected by a 2D matrix-detector with 256×256 pixels, each with surface area of 2.2×2.2 mm². The measurement were performed at $T = 22$ °C.

3. RESULTS AND DISCUSSION

3.1. Light-optical diffraction

Fig. 2 shows angular dependences of the intensity of the 0th and the -1st diffraction orders for $\lambda_R = 543$ nm measured 3°C above the N-I phase transition temperature T_c . The rotation angle θ is given with respect to the normal incidence of the probe beam. The intensities are given relative to that of the incident beam, renormalized for reflection losses at normal incidence. The vertical dashed line denotes Bragg angle incidence. The results obtained for *s*- (parallel to *y*-axis) and for *p*- (within the *xz* plane) polarized beams are identical. This indicates that above T_c the grating is completely optically isotropic, i.e., the amplitude of the refractive-index modulation is independent of the polarization of the optical beam.

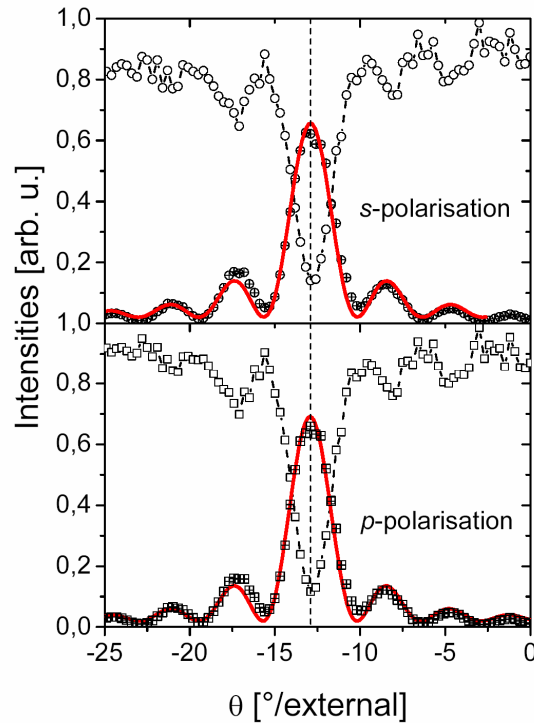


Fig. 2. Angular dependencies of the 0th (open symbols) and the -1st (crossed symbols) order diffraction intensities measured at 3 °C above the nematic-isotropic phase transition. Solid lines are fits according to Eq. (2).

The optical diffraction efficiency (defined as a ratio between the diffracted and the incident intensity I_{in}) of a lossless volume phase grating having a sinusoidal refractive-index profile $n(x)$ with the spatial frequency $K_g = |\mathbf{K}_g| = 2\pi/\Lambda$ of the grating vector (Fig. 1), which is described by

$$n(x) = n_0 + n_1 \cos(K_g x), \quad (1)$$

is given as^{6,7}:

$$\eta(\nu, \xi) = \frac{\sin^2 \sqrt{\nu^2 + \xi^2}}{1 + \xi^2 / \nu^2}. \quad (2)$$

Here d is the thickness, $\nu = \pi n_1 d / (\lambda \cos \theta)$ is the grating strength and $\xi = \Delta \theta \pi d / \lambda$ is a measure for the deviation from the Bragg condition, i.e., $\Delta \theta = \theta - \theta_B$. The values of θ in these relations are associated with the beam propagation within the H-PDLC medium. The Bragg angle is given by $2n_0 \sin \theta_B = \lambda_R / \Lambda$, where λ_R is the wavelength of the probe beam in free space. A fit of Eq. (2) to the experimental data shown in Fig. 2 results in $\nu_s = 1.89 \pm 0.03$ and $\nu_p = 1.84 \pm 0.03$ for s - and p -polarization, while the obtained values for the grating thickness and grating spacing are $d = 30.5 \pm 0.4 \mu\text{m}$ and $\Lambda = 1.20 \pm 0.02 \mu\text{m}$, respectively. The resolved value of d is 40% smaller than the thickness of the plastic spacers L , which is attributed to the formation of surface layers of pure polymer, which takes place due to hampering of the photoinitiator at the surfaces. A presence of such surface layers was revealed by the scanning electron microscopy (SEM) analysis.

The measured values of ν_s and ν_p give optical refractive index parameters $n_0 = 1.52 \pm 0.01$ and $n_1 = 0.011 \pm 0.001$ (see Eq. (1)). The modulation n_1 is a consequence of the refractive-index mismatch between the polymer rich and the LC rich regions. If one assumes that the LC rich regions are composed only of the LC material and the fluoro-additive, then according to the volume fraction of the compounds the refractive index of these regions is expected to be $n_{LCr} = 1.549$ (at $\lambda = 598 \text{ nm}$). On the other hand, if the polymer rich regions were layers of a pure polymer, their refractive index would be $n_p = 1.473$. The expected modulation for this extreme case is $n_{1,\text{max}} = 0.038$. The obtained 3.5 times lower value indicates that the ingredients of our sample are still quite far from being completely unmixed and separated into slices, which is in agreement with the profound light scattering observed in the nematic phase, which indicates the presence of numerous LC droplets.

Below the N-I phase transition temperature the optical diffraction properties of the gratings become much more intricate. The grating strength for p -polarization is much higher than for s -polarization. Besides this, the shape of the angular dependence is strongly smeared out as compared to theory due to the scattering effects. These features are related to the complex structure of the nematic director field within the LC domains and are described in more details elsewhere⁸.

3.2. Neutron-optical diffraction

Coherent elastic scattering of nonrelativistic particles, such as cold neutrons with wavelengths of $0.5 \text{ nm} < \lambda_n < 5 \text{ nm}$, can be described rigorously by a one-body, time-independent Schrödinger equation⁹. The latter governs all neutron-optical phenomena and the scalar wave equation is exactly the same as for light optics, provided that the refractive index n_n for neutrons is defined as⁹

$$n_n(x) = \sqrt{1 - \frac{V(x)}{E}} \approx \left(1 - \frac{V(x)}{2E}\right), \quad (3)$$

where E is the total energy of the particle and $V(x)$ is neutron-optical potential. Due to the extremely short interaction lengths of cold neutrons with atomic nuclei, $V_n(x)$ is usually replaced by a series of Fermi pseudopotentials

$$V_n(x) = \frac{\hbar^2}{2\pi m} \sum_j b_j \delta(x - y_j) = \frac{\hbar^2}{2\pi m} b^\rho(x), \quad (4)$$

where \hbar is Planck's constant and m the neutron mass. The summation takes place over the different nuclei j with scattering length b_j located at the corresponding sites y_j , while $b^\rho(x)$ denotes the so-called coherent scattering length density. By assuming that internal degrees of freedom of atoms are statistically independent of their positions, $b^\rho(x)$ can be simplified to

$$b^\rho(x) = [\bar{b}N](x), \quad (5)$$

where \bar{b} is the bound scattering length averaged over a unit, e.g., a unit cell in a regular crystal or a polymer unit, and N is the number density. In grating structures formed from pure photopolymer materials, the first term in Eq. (5) is constant and only density variations affect neutron diffraction. In case of composite media, which exhibit phase separation of the

constituent components, also \bar{b} becomes spatially dependent and so larger variations of b^ρ can be induced. According to Eq.(3)-Eq.(5) it follows

$$n_n(x) = \frac{\lambda_n^2}{2\pi} b^\rho(x). \quad (6)$$

Due to the periodic modulation of the material composition in a H-PDLC transmission grating, its spatial variation of the refractive index for neutrons can be described analogously to the case of the light-optical refractive index modulation, i.e. by Eq. (1). The corresponding modulation parameter n_1 for neutrons is given as

$$n_{1n} = \frac{\lambda_n^2}{2\pi} \Delta(\bar{b}N) = \frac{\lambda_n^2}{2\pi} b_1^\rho, \quad (7)$$

where b_1^ρ denotes the scattering contrast. Despite the analogous form of the refractive-index modulation, however, aside their different interaction potentials there is another significant difference between light and neutron diffraction. Due to the much lower wavelength of neutrons, the diffraction regimes for the two cases are quite different. While for light the diffraction gratings under investigation can be well described as volume gratings, for which the diffraction process is based on two-wave coupling (Eq. (2)), neutrons in the same structure exhibit multiple beam coupling and hence the rigorous coupled-wave theory should be used to explain their diffraction features^{10,11}.

Fig. 3 shows the angular dependence of the $\pm 1^{\text{st}}$ order diffraction efficiencies of an H-PDLC grating observed for a central neutron wavelength of $\lambda_n = 1.16$ nm. The corresponding Bragg angle $\theta_{\text{Bn}} = \sin^{-1}(\lambda_n/2A)$ is 0.48 mrad and consequently the two peaks exhibit maxima practically at normal incidence. From the FWHM of the diffraction peaks, which is about 40 mrad, we find the effective thickness of the grating $d=(A/\text{FWHM})=30$ μm , which is in good agreement with the value deduced from the light diffraction measurements. Because the maximal diffraction efficiency $\eta_{\pm 1}$ is only 3%, higher diffraction orders are very weak and consequently the two-wave coupling (Eq. 2) can be used as a reasonable approximation of the observed behaviour. A fit of Eq. (2) to the experimental data results in $n_{1n} = (2.12 \pm 0.05) \cdot 10^{-6}$ and correspondingly $b_1^\rho = (9.89 \pm 0.26) \cdot 10^{12}$ m^{-2} . These values are nearly two orders of magnitude larger as compared to that of any photo-neutron-refractive material probed up to now¹.

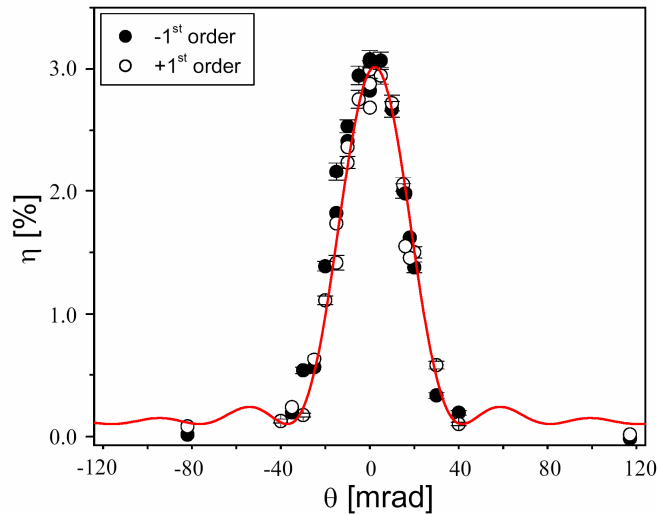


Fig. 3. Angular dependence of the $\pm 1^{\text{st}}$ order diffraction efficiencies for neutrons at $\lambda_n = 1.16$ nm. Solid line represents a fit to Eq. (2).

If one assumes a complete phase separation into the slice-like structure, a maximal possible value of n_{1n} can be calculated from the known chemical composition and density of the constituent compounds. However, due to the limited

information available on the composition of the commercial mixtures used for our samples, only a rough estimation could have been made. It follows, that the maximum achievable contrast for the first Fourier component of the neutron refractive index modulation of our material is $n_{1n,max} \sim 13 \cdot 10^{-6}$, which is 6 times larger from the experimentally observed value. This again signifies that in our samples the LC and the polymer material are still quite far from being completely phase separated.

4. CONCLUSIONS

We demonstrated that H-PDLCs with a thickness of only 30 μm act as extremely efficient gratings not only for light, but also for neutrons. The modulation of the neutron optical potential attains the value of nearly 10% of the average particle potential. Due to the high modulation amplitude and low sample thickness, incoherent neutron scattering has minor influence on the sample transmission, so that no material deuteration is needed. This strongly reduces the costs for fabrication of potential devices, hence H-PDLCs are very prospective as new materials for application in various neutron-optical elements for cold and ultracold neutrons. In this respect we should mention that the H-PDLC mixture used in our experiments has been optimized for light, not for neutron diffraction. Therefore we believe that with optimization of the material composition and structure in view of neutron refractive-index contrast, further increase of the modulation for an order of magnitude is feasible.

ACKNOWLEDGMENTS

We acknowledge the financial support of the ÖAD in the frame of the STC program Slovenia-Austria (SI-A4/0708) and the Austrian Science fund FWF (P-18988).

REFERENCES

1. M. Fally, *Appl. Phys. B* **75**, 405-426 (2002); M. Fally, C. Pruner, R. A. Rupp, G. Krexner, *Neutron Physics with Photorefractive Materials in Springer Series of Optical Sciences* **115**, eds. P. Günter and J.-P. Huignard, Springer Verlag, 2007.
2. T. Bunning, L.V. Natarjan, V. P. Tondiglia, and R. L. Sutherland, *Ann. Rev. Mater. Sci.* **30**, 83 (2000).
3. G. P. Crawford, *Optics and Photonics News* **14**, 54 (2003).
4. C.C. Bowley and G. P. Crawford, *Appl. Phys. Lett.* **76**, 2235 (2000).
5. I. Drevenšek-Olenik, M. Jazbinšek, M. E. Sousa, A. K. Fontecchio, G. P. Crawford, M. Čopič, *Phys. Rev. E* **69**, 051703 (2004).
6. P. Hariharan, *Optical Holography: Principles, Techniques and Applications*, 2nd Ed., Cambridge University Press, 1996.
7. H. Kogelnik, *Bell Syst. Tech. J.* **48**, 2909 (1969).
8. I. Drevenšek-Olenik, M. Fally, M. A. Ellabban, *Phys. Rev. E* **74**, 021707 (2006).
9. V. F. Sears, *Neutron Optics*, Vol. 3 of *Neutron scattering in condensed matter*, eds. S. W. Lovesey and E. W. Mitchell, Oxford University Press, 1989.
10. M. G. Moharam, T. K. Gaylord, *J. Opt. Soc. Am.* **71**, 811 (1981).
11. M. Fally, I. Drevenšek-Olenik, M. A. Ellabban, K. P. Pranzas, J. Vollbrandt, *Phys. Rev. Lett.* **97**, 167803 (2006).